ARTICLES

Journal of Semiconductors
(2021) 42, 062302
doi: 10.1088/1674-4926/42/6/062302

Heavily doped silicon: A potential replacement of conventional plasmonic metals

Md. Omar Faruque†, Rabiul Al Mahmud, and Rakibul Hasan Sagor

Islamic University of Technology (IUT), Board Bazar Gazipur, Gazipur 1704, Bangladesh

Abstract: The plasmonic property of heavily doped p-type silicon is studied here. Although most of the plasmonic devices use metal–insulator–metal (MIM) waveguide in order to support the propagation of surface plasmon polaritons (SPPs), metals that possess a number of challenges in loss management, polarization response, nanofabrication etc. On the other hand, heavily doped p-type silicon shows similar plasmonic properties like metals and also enables us to overcome the challenges possessed by metals. For numerical simulation, heavily doped p-silicon is mathematically modeled and the theoretically obtained relative permittivity is compared with the experimental value. A waveguide is formed with the p-silicon-air interface instead of the metal–air interface. Formation and propagation of SPPs similar to MIM waveguides are observed.

Key words: alternative plasmonic material; heavily doped p-silicon; surface plasmon polaritons

Citation: M O Faruque, R Al Mahmud, and R H Sagor, Heavily doped silicon: A potential replacement of conventional plasmonic metals[J]. *J. Semicond.*, 2021, 42(6), 062302. http://doi.org/10.1088/1674-4926/42/6/062302

1. Introduction

Optical waveguide devices are making their way towards realizing low-cost high sensitivity and small-size devices, leading to many applications such as biological, environmental and chemical applications[1–3]. Most of these waveguide devices use a metal-insulator-metal (MIM) waveguide to guide SPPs. Although metals such as gold and silver are mostly used in plasmonic devices due to their small ohmic losses and ability to confine light within considerable propagation length[4], at optical frequencies, metals suffer a huge optical loss due to interband transitions[5]. Natural metals also have a large real part of its complex dielectric permittivity compared to dielectric, which causes a lot of problems in plasmonic devices that require a nearly balanced polarization response[6]. Besides, the optical properties of metals degrade to a large extent when manufactured as thin films because metal films have different morphologies compared to a bulk metal[7].

To overcome the above-mentioned limitations of metals, another alternative material is proposed here which can support SPP propagation like natural metals. The plasmonic properties of natural metals can be described by its dielectric permittivity, ε, and magnetic permeability, μ. At optical frequencies, magnetic permeability, μ, is close to unity. Thus, the optical behavior can fully be described by the dielectric permittivity, ε[8]. The complex dielectric permittivity of metals has a negative real part and a positive imaginary part. Both the real part and imaginary part is large in magnitude due to their high carrier concentration ($\approx 10^{23}$ cm^{-3}). The large real part of the dielectric permittivity compared to the dielectric permittivity of the insulator causes an unbalanced polarization response in the MIM waveguide[9]. Also, the large value of imaginary part is the reason for a comparatively higher optical loss. Thus, smaller values of both the real part and imaginary part of the dielectric permittivity of metal would have been advantageous for the plasmonic applications.

Silicon, when doped over a certain carrier concentration, shows negative real permittivity just like metals. Thus, it can support SPP propagation at its interface with a dielectric. So, it can be used to replace metals in the MIM structure. Both the real part and imaginary part of the permittivity depends on the carrier concentration which is tunable in this case of doped silicon and thus can be reduced to a certain limit to make the permittivity values smaller. Thus, both polarization management and optical loss can be controlled to a great extent. For the process of nanofabrication, silicon on insulator (SOI) is one of the key technologies nowadays. Since this kind of waveguide has only silicon in its structure, it can be treated in the same way as SOI structures. This will make the structure complementary metal oxide semiconductor (CMOS)-compatible and thus, will provide an easier way of fabrication.

2. Theoretical modeling of doped silicon

The p-silicon used here must be doped up to a certain carrier concentration in order to make it behave like metals. For our design, it is assumed to be doped in the range of 10^{20} to 10^{21} cm^{-3}. Carrier concentration in this range has been practically shown by Shahzad *et al.*[9], Linaschke *et al.*[10], Mizushima *et al.*[11], Vina *et al.*[12], Ma *et al.*[13], Miyao *et al.*[14] and Jellison Jr *et al.*[15]. The highest carrier concentration of 2×10^{22} in silicon has been reported by Nobili *et al.*[16]. The complex relative permittivity of highly doped silicon can be described by the Lorentz-Drude model[17].

$$\varepsilon(\omega) = \varepsilon_\infty - \omega_p^2 / \{\omega^2[1 + i(1/\omega\tau)]\}. \tag{1}$$

If the real part and imaginary parts are separated, Eq. (1) becomes

Correspondence to: M O Faruque, omarfaruque@iut-dhaka.edu
Received 26 SEPTEMBER 2020; Revised 5 JANUARY 2021.
©2021 Chinese Institute of Electronics

Table 1. Modelling parameters of heavily doped p-silicon by the Lorentz-Drude model.

Parameter	Value for carrier concentration of 6×10^{19} cm^{-3}	Value for carrier concentration of 1×10^{20} cm^{-3}
ε_0	11.7	11.7
e	1.60217662×10^{-19}	1.60217662×10^{-19}
μ	50	50
$m_{\rm eff}$	$3.5526595884\times10^{-31}$	$3.5526595884\times10^{-31}$
τ	$1.2417416061807\times10^{-10}$	$1.241741606180\times10^{-10}$
σ	5.3833134432×10^{8}	8.972189072×10^{8}

$$\varepsilon(\omega)=\left(\varepsilon_\infty-\omega_{\rm p}^2\tau^2/1+\omega^2\tau^2\right)+i\left[\omega_{\rm p}^2\tau/\omega\left(1+\omega^2\tau^2\right)\right], \quad (2)$$

where $\omega_{\rm p}$ is the plasma frequency, ε_∞ is the infinite frequency relative permittivity or the background permittivity, τ is the electron/hole relaxation time, $\omega = 2\pi c/\lambda$ is the angular frequency, c is the speed of light in vacuum and i is the imaginary unit. In the case of the highly doped degenerate intrinsic semiconductors, $\omega_{\rm p}^2 = Ne^2/\varepsilon_0 m_{\rm eff}$ and $\tau = \mu m_{\rm eff}/e$, where N is the free carrier concentration, μ is the electron/hole's drift mobility and $m_{\rm eff}$ is the averaged electron/hole effective mass[18]. Usually, the angular frequency $\omega \gg \omega_{\rm p}$ and $\omega\tau \gg 1$[19]. Thus, Eq. (2) can be rewritten as

$$\varepsilon(\omega)=[\varepsilon_\infty-(\sigma/\omega^2\varepsilon_0\tau)]+i(\sigma/\omega^3\tau^2\varepsilon_0), \quad (3)$$

where $\sigma \approx eN\mu$ is the conductivity of the doped silicon and e is the charge of an electron and ε_0 is the free space permittivity. The infinite frequency relative permittivity or the background permittivity is the high-frequency limiting value that is approximately 11.7 for silicon and is independent of the doping concentration[20, 21]. Here, μ = 50[22] and $m_{\rm eff}$= 0.37m_0, where m_0 is the mass of the electron[23]. The real part of the complex permittivity becomes negative after a certain concentration which can be calculated using Eq. (3). The values of different parameters of (3) for p-silicon carrier concentration of 6×10^{19} and 1×10^{20} cm^{-3} is shown in Table 1.

The relative permittivity of heavily doped p-silicon has been experimentally measured by Shahzad *et al.* [9] for carrier concentration of 6×10^{19} and 1×10^{20} cm^{-3}. Comparison between the values calculated from Eq. (3) and the experimental value for carrier concentration of 6×10^{19} and 1×10^{20} cm^{-3} has been shown in Fig. 1.

The percentages of error between the theoretically calculated value using the Lorentz-Drude model and the experimentally obtained value by Shahzad *et al.* at different wavelengths for p-silicon carrier concentration of 6×10^{19} and 1×10^{20} cm^{-3} has been shown in Tables 2 and 3, respectively.

From Fig. 1 and Table 2, it is observed that for a carrier concentration of 6×10^{19} cm^{-3}, the percentage of error between the theoretical value and the experimental value is very high (>160%) for wavelengths greater than 9.69 μm, high (40%) for wavelengths between 6.5 to 9.69 μm and very low ($\leqslant$ 3.95%) for wavelengths less than 6.5 μm. For a carrier concentration of 1×10^{20} cm^{-3}, the percentage of error is very high (>109.7%) for wavelengths greater than 26.23 μm, high (20.35%–34.33%) for wavelengths between 3.86 to 17.69 μm and low ($\leqslant$ 7.12%) for wavelengths smaller than 3.34 μm.

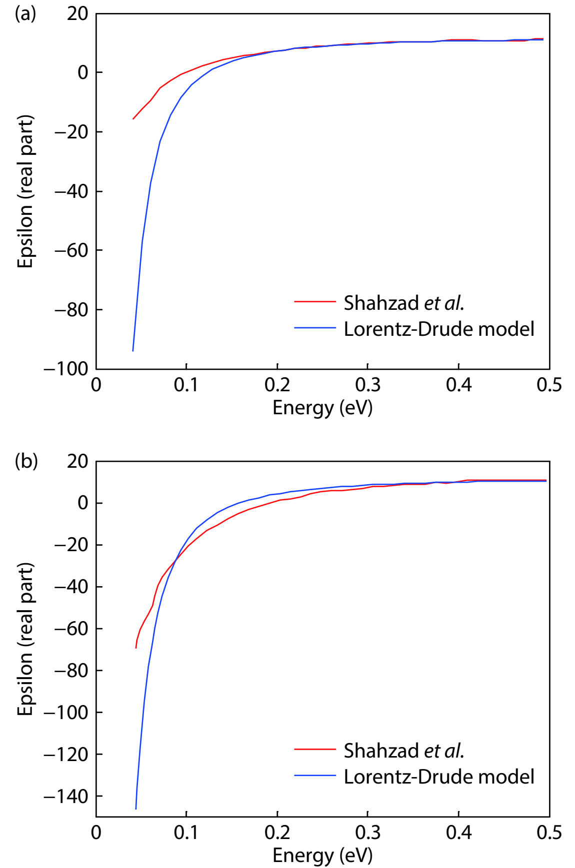

Fig. 1. (Color online) Comparison between theoretical value and experimental value for carrier concentration of (a) 6×10^{19} cm^{-3} and (b) 1×10^{20} cm^{-3}.

The Lorentz-Drude model mainly provides the frequency dependent dielectric permittivity of metals. In metals, electronic transition from the valence band to the conduction band takes place at a lower photon energy which is taken into consideration while theoretical modeling of any material is done using the Lorentz-Drude model. However, the band structure possessed by semiconductors like silicon is quite different compared to those of metals and the energy gap between the conduction band and valence band is also higher in semiconductors compared to metals. Thus, at lower photon energy, the dielectric property of doped silicon given by the Lorentz-Drude model, considering the contribution from interband transition of electrons, does not match with the experimental result as there is no interband transition practically. However, at higher photon energy, electrons in the semiconductor can absorb the required energy for interband transition just like metals. Thus, at higher photon energy, the Lorentz-Drude model can provide us with the more accurate values since the theoretical assumption regarding the interband transition also takes place practically. This difference in the theoretically predicted value and the experimentally obtained value at low photon energy has been depicted in Fig. 1. At higher photon energy, the theoretical and experimental value matches with each other as predicted by the theory. Analyzing the data from Tables 2 and 3, it is evident that the model shows a low percentage of error for wavelengths smaller than 3.34 μm. Thus, this model of heavily doped p-silicon can be used for the plasmonic devices, which work in the range of wavelengths smaller

Table 2. Comparison of relative permittivity of p-silicon between the theoretical value and the experimental value for a carrier concentration of 6×10^{19} cm^{-3}.

Energy (eV)	Wavelength (μm)	Values of relative permittivity (real part)		Percentage of error (%)
		Experimental (Shahzad *et al.*[9])	Theoretical (Lorentz-Drude model)	
0.14	8.1	4.43	2.64	40
0.15	7.49	4.95	3.97	19.88
0.16	6.96	5.53	5.02	9.27
0.17	6.5	6.12	5.87	3.95
0.28	4.08	9.67	9.4	2.84
0.35	3.27	10.41	10.22	1.83
0.42	2.73	10.82	10.67	1.45
0.45	2.52	10.71	10.82	1.02

Table 3. Comparison of relative permittivity of p-silicon between the theoretical value and the experimental value for a carrier concentration of 1×10^{20} cm^{-3}.

Energy (eV)	Wavelength (μm)	Values of relative permittivity (real part)		Percentage of error (%)
		Experimental (Shahzad *et al.*[9])	Theoretical (Lorentz-Drude model)	
0.064	17.69	−44.85	−60.24	34.33
0.067	16.72	−39.97	−52.62	31.66
0.11	10.23	−17.14	−12.40	27.60
0.29	3.86	6.88	8.29	20.35
0.30	3.71	7.56	8.53	12.86
0.34	3.34	8.53	9.14	7.12
0.43	2.63	10.81	10.11	6.43
0.46	2.49	10.81	10.27	4.98

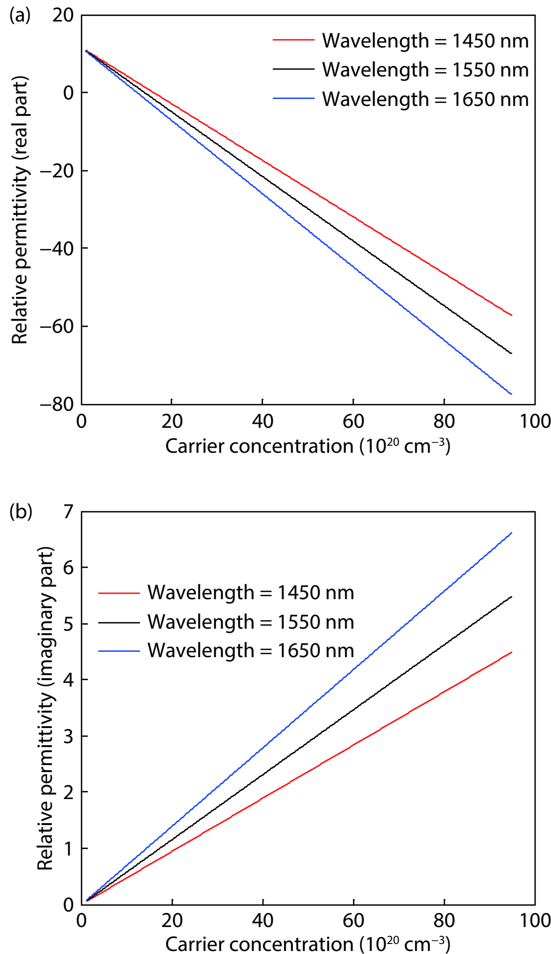

Fig. 2. (Color online) Relative permittivity (a) real part and (b) imaginary part versus carrier concentration at different wavelength.

than 3.34 μm, which is the case for most of the plasmonic applications.

Heavily doped p-silicon can also be modeled at other carrier concentrations and wavelengths. The relationship of both the real part and imaginary part of the permittivity with carrier concentration and wavelength is almost linear. Fig. 2 shows the plot of relative permittivity against carrier concentration for different wavelengths.

3. Comparison with conventional plasmonic metals

Among the conventional plasmonic materials, gold and silver are the most commonly used metals. A number of models for gold and silver are already available for use. The complex dielectric permittivity of gold and silver has been determined using both the Drude model and Lorentz-Drude model considering the effect of both free electrons and bound-electrons in metals. The part on which free-electron effects act $\varepsilon_r^{(f)}(\omega)$, can be expressed in the following form:

$$\varepsilon_r^{(f)}(\omega) = 1 - \frac{\Omega_p^2}{\omega(\omega - i\Gamma_0)}, \tag{4}$$

and the part on which bound-electron effects act $\varepsilon_r^{(b)}(\omega)$, can be described by the Lorentz model in the following form:

$$\varepsilon_r^{(b)}(\omega) = \sum_{n=1}^{k} \frac{f_n \omega_p^2}{(\omega_n^2 - \omega^2) + i\omega\Gamma_n}, \tag{5}$$

where ω_p refers to the plasma frequency, k refers to the number of oscillation with resonance frequency ω_n, dominant frequency f_n, damping frequency Γ_n and $1/\Gamma_n$ is the lifetime. Here Ω_p refers to the plasma frequency of the free-electron

Table 4. Modelling parameters of gold and silver by the Drude and Lorentz-Drude model.

Parameter	Value for silver (eV)	Value for gold (eV)
Plasma frequency ($\hbar\omega_p$)	9.01	9.03
Damping constant (Γ_0)	0.048	0.053
Oscillator strength (f_0)	0.845	0.760
Dominant frequency(f_n)	[0.065; 0.011; 0.840; 5.646]	[0.024; 0.010; 0.071; 0.601; 4.384]
Damping frequency (Γ_n)	[3.886; 0.452; 0.065; 0.916; 2.419]	[0.241; 0.345; 0.870; 2.494; 2.214]
Resonance frequency (ω_n)	[0.816; 4.481; 8.185; 9.083; 20.29]	[0.415; 0.830; 2.969; 4.304; 13.32]
Number of resonance	6	6

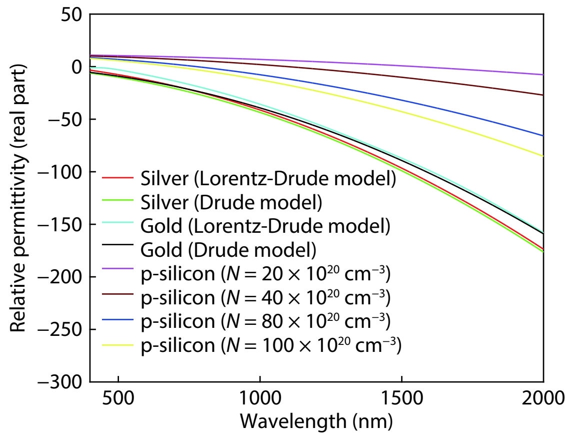

Fig. 3. (Color online) Real part of relative permittivity for silver, gold and, p-silicon for different values of carrier concentration of p-silicon.

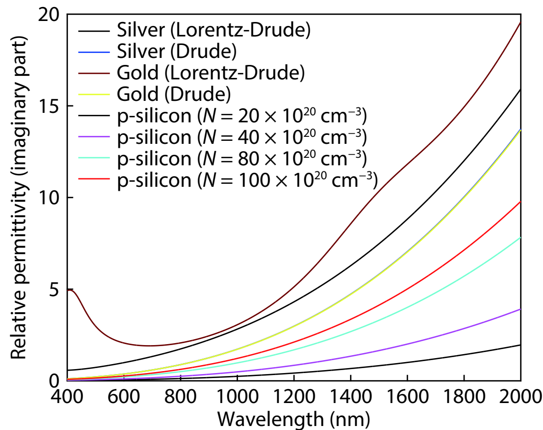

Fig. 4. (Color online) Imaginary part of relative permittivity for silver and gold, and p-silicon for different values of carrier concentration.

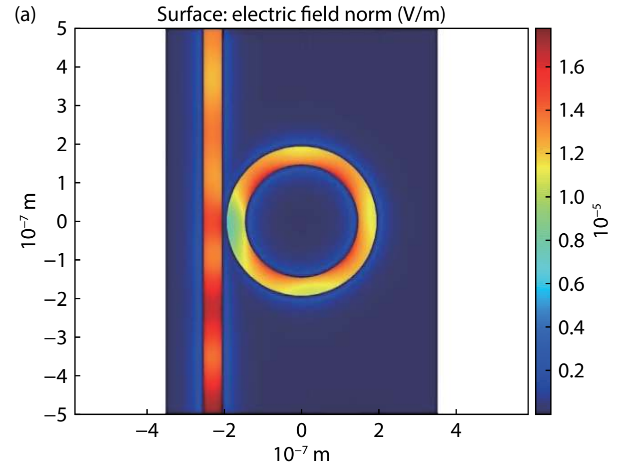

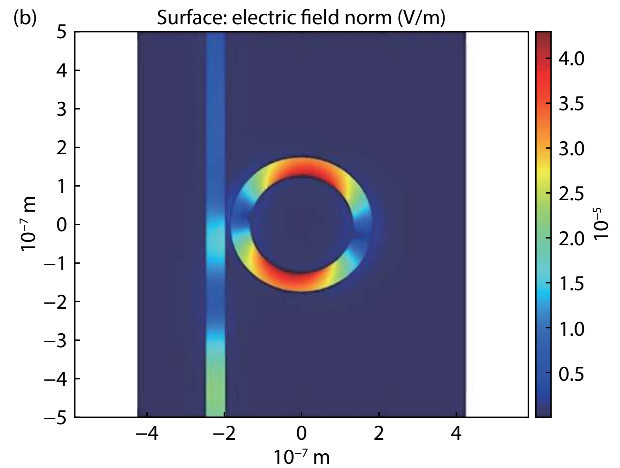

Fig. 5. (Color online) Propagation of SPP along the silicon–air–silicon waveguide.

model having damping constant Γ_0 and oscillator strength f_0. Finally, the complex dielectric function can be described in the following form:

$$\varepsilon_r(\omega) = \varepsilon_r^{(f)}(\omega) + \varepsilon_r^{(b)}(\omega). \quad (6)$$

Values of different parameters for obtaining the permittivity of gold and silver have been reported by Rakic *et al.*[24], which are shown in Table 4.

Since the relative permittivity is a complex quantity, it will have both real and imaginary parts. Fig. 3 shows the real part of both gold and silver plotted along with the real part of the permittivity of p-silicon for different carrier concentration.

From Fig. 3, it is observed that silver, gold and p-silicon, all have negative real parts of the permittivity after a certain wavelength. The real part of the complex permittivity for both gold and silver is larger than the p-silicon. This is mainly due to their high carrier concentration (≈10^{23} cm^{-3}). The large real part of the permittivity causes polarization mismatch in many plasmonic devices when the interface is created with an insulator[20, 25, 26]. Thus, it is desirable to have smaller value of real permittivity for having a balanced polarization response. Since p-silicon has a comparatively smaller real part, it will be advantageous in forming plasmonic devices compared to both gold and silver.

Comparison between the imaginary parts of the dielectric permittivity is shown in Fig. 4. The imaginary parts of the permittivity of both gold and silver are much larger than that of p-silicon even at a higher carrier concentration of p-silicon. Since the large value of the imaginary part is responsible for larger optical loss, plasmonic devices formed with p-silicon will suffer much lower optical loss than the conventional met-

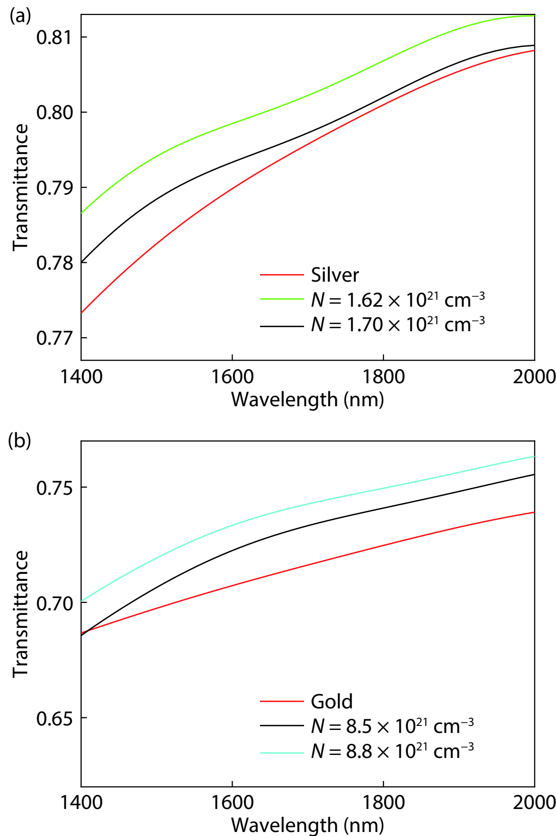

Fig. 6. (Color online) Comparison of the transmittance between (a) the silver and p-silicon waveguide and (b) the gold and p-silicon waveguide.

al plasmonic devices.

4. Waveguide formation and result analysis

A straight waveguide with a ring resonator is formed with a silicon–insulator–silicon structure instead of MIM. The waveguide is simulated and SPP propagation similar to the MIM waveguide is observed. For simulation purposes, commercial simulation software COMSOL Multiphysics was used. Fig. 5 shows the normalized electric field distribution at wavelength 1400 and 1800 nm respectively for the ring resonator structure formed with the silicon-air-silicon waveguide. From Fig. 5, it is clearly observable that SPPs are created and propagated along the interface of p-silicon and air. Thus, we can come to a conclusion that p-silicon can be used as a replacement of metal in plasmonic devices in order to support SPP propagation.

The comparison of the transmittance in a straight waveguide formed with silver-air-silver and gold-air-gold with the same structure formed with a silicon-air-silicon waveguide with different carrier concentration is shown in Fig. 6 which shows that, by doping the silicon up to a certain concentration, transmittance more than both the silver-air-silver and gold-air-gold can be achieved. The doped silicon waveguide can also be used to obtain transmission response of a notch filter similar to those of MIM waveguides by coupling the straight waveguide with a ring resonator as shown in Fig. 5. The notch type response of the ring resonator structure with MIM waveguides and doped silicon waveguide is shown in Fig. 7. The sensing characteristics of the ring resonator with doped silicon can be utilized to use it as a refractive index sensor by placing the sensing material in the ring waveguide.

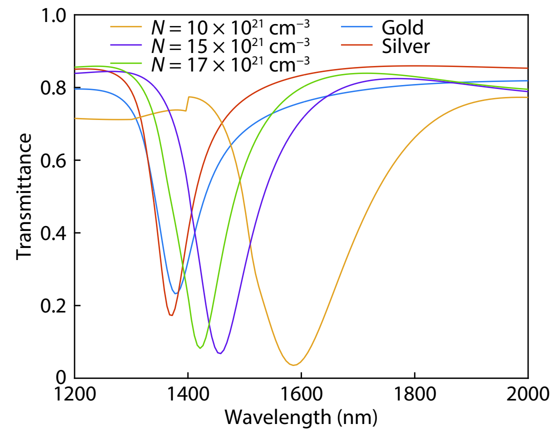

Fig. 7. (Color online) Notch type transmission response shown by ring resonators using gold, silver and psilicon.

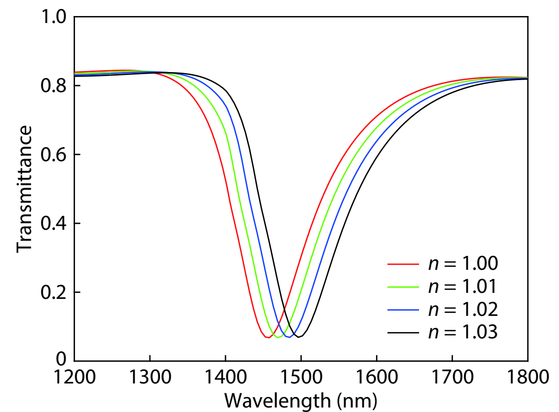

Fig. 8. (Color online) Sensing characteristics shown by ring resonators formed with heavily doped silicon.

The resonant wavelength shifts with the change of refractive index, n, of the sensing material which is shown in Fig. 8. Similarly, in most of the plasmonic devices, the metals like gold and silver can be replaced by doped silicon of the required carrier concentration to enhance the performance of the devices and to provide a more suitable way of fabrication.

5. Conclusion

A potential replacement of metals in plasmonic devices, heavily doped p-silicon is modeled here. The modeling parameters are found out for different carrier concentrations of p-silicon and the result is compared with the experimentally obtained result for the carrier concentration of 6×10^{19} and 1×10^{20} cm^{-3}. In both cases, the error percentage for wavelengths smaller than 3.34 μm has been found to be $\leqslant$ 7.12% which trends to decrease gradually as the wavelength becomes smaller, since most of the plasmonic devices operate in the range of wavelengths smaller than 2 μm where the error percentage is expected to be much less than the error obtained here. Thus, the mathematical model can be considered as verified one for wavelengths smaller than 3.34 μm. The real part of the relative permittivity obtained in the model shows negative permittivity for a carrier concentration greater than 23×10^{20} cm^{-3}. Thus, it will behave like metal after doping with a carrier concentration of than 23×10^{20} cm^{-3} and can be used in plasmonic devices instead of metal to guide SPPs, which is also observed here by simulation. Hence, we can come to a conclusion that heavily

doped p-silicon can behave like metal and can be used as a replacement of metals in plasmonic devices which will help us to overcome optical loss, unbalanced polarization response and nanofabrication challenges possessed by metals.

References

[1] Barnes W L, Dereux A, Ebbesen T W. Surface plasmon subwavelength optics. Nature, 2003, 424, 824

[2] Lu H, Liu X, Wang G, et al. Tunable high-channel-count bandpass plasmonic filters based on an analogue of electromagnetically induced transparency. Nanotechnology, 2012, 23, 444003

[3] Wang H Q, Yang J B, Zhang J J, et al. Tunable band-stop plasmonic waveguide filter with symmetrical multiple-teeth-shaped structure. Opt Lett, 2016, 41, 1233

[4] Johnson P B, Christy R W. Optical constants of the noble metals. Phys Rev B, 1972, 6, 4370

[5] West P R, Ishii S, Naik G V, et al. Searching for better plasmonic materials. Laser Photonics Rev, 2010, 4, 795

[6] Cai W S, Chettiar U K, Kildishev A V, et al. Optical cloaking with metamaterials. Nat Photonics, 2007, 1, 224

[7] Abelès F, Borensztein Y, López Rios T. Optical properties of discontinuous thin films and rough surfaces of silver. In: Advances in Solid State Physics. Berlin, Heidelberg: Springer Berlin Heidelberg, 2007, 93

[8] Berestetskii V B, Lifshitz E M, Pitaevskii L P. Quantum Electrodynamics. Volume 4. Butterworth-Heinemann, 1982

[9] Shahzad M, Medhi G, Peale R E, et al. Infrared surface plasmons on heavily doped silicon. J Appl Phys, 2011, 110, 123105

[10] Linaschke D, Schilling N, Dani I, et al. Highly n-doped surfaces on n-type silicon wafers by laser-chemical processes. Energy Procedia, 2014, 55, 247

[11] Mizushima I, Murakoshi A, Watanabe M, et al. Hole generation without annealing in high dose boron implanted silicon: Heavy doping by B12 icosahedron as a double acceptor. Jpn J Appl Phys, 1994, 33, 404

[12] Viña L, Cardona M. Effect of heavy doping on the optical properties and the band structure of silicon. Phys Rev B, 1984, 29, 6739

[13] Ma Z, Liu Y, Deng L, et al. Heavily boron-doped silicon layer for the fabrication of nanoscale thermoelectric devices. Nanomaterials, 2018, 8, 77

[14] Miyao M, Motooka T, Natsuaki N, et al. Change of the electron effective mass in extremely heavily doped n-type Si obtained by ion implantation and laser annealing. Solid State Commun, 1981, 37, 605

[15] Jellison G E, Modine F A, White C W, et al. Optical properties of heavily doped silicon between 1.5 and 4.1 eV. Phys Rev Lett, 1981, 46, 1414

[16] Nobili, Solmi, Parisini, et al. Precipitation, aggregation, and diffusion in heavily arsenic-doped silicon. Phys Rev B, 1994, 49, 2477

[17] Maier S A. Spectroscopy and sensing. In: Plasmonics: Fundamentals and Applications. New York, NY: Springer US, 2007, 177

[18] Saber M G, Abadía N, Plant D V. CMOS compatible all-silicon TM pass polarizer based on highly doped silicon waveguide. Opt Express, 2018, 26, 20878

[19] Qi Z P, Hu G H, Li L, et al. Design and analysis of a compact SOI-based aluminum/highly doped p-type silicon hybrid plasmonic modulator. IEEE Photonics J, 2016, 8, 1

[20] Naik G V, Shalaev V M, Boltasseva A. Alternative plasmonic materials: Beyond gold and silver. Adv Mater, 2013, 25, 3264

[21] Chen Y B, Zhang Z M. Heavily doped silicon complex gratings as wavelength-selective absorbing surfaces. J Phys D, 2008, 41, 095406

[22] Schroder D K, Thomas R N, Swartz J C. Free carrier absorption in silicon. IEEE J Solid-State Circuits, 1978, 13, 180

[23] van Exter M, Grischkowsky D. Carrier dynamics of electrons and holes in moderately doped silicon. Phys Rev B, 1990, 41, 12140

[24] Rakić A D, Djurišić A B, Elazar J M, et al. Optical properties of metallic films for vertical-cavity optoelectronic devices. Appl Opt, 1998, 37, 5271

[25] Kildishev A V, Shalaev V M. Engineering space for light via transformation optics. Opt Lett, 2008, 33, 43

[26] Cai W S, Chettiar U K, Kildishev A V, et al. Designs for optical cloaking with high-order transformations. Opt Express, 2008, 16, 5444

Md. Omar Faruque completed his B.Sc. in 2016 and M.Sc. in 2019 in Electrical and Electronic Engineering from the Islamic University of Technology (IUT), Gazipur, Bangladesh. He joined as a Lecturer in the Department of Electrical and Electronic Engineering of the Islamic University of Technology (IUT), Gazipur, Bangladesh, a subsidiary organ of OIC in Bangladesh, in 2017 and serving there to date. Plasmonic metamaterials, plasmonic devices and integrated optical systems are notable in his current research interests.

Rabiul Al Mahmud is currently Lecturer at the Department of Electrical and Electronic Engineering at the Islamic University of Technology (IUT), Gazipur, Bangladesh, a subsidiary organ of OIC in Bangladesh. He obtained the B.Sc. and M.Sc. degree in Electrical and Electronic Engineering from the Islamic University of Technology (IUT), Gazipur, Bangladesh, in 2016 and 2020 respectively. His areas of interests are plasmonics, plasmonic devices and materials. He has published four research papers in referred journals and conference proceedings like IEEE, Springer and Elsevier.

Rakibul Hasan Sagor received a B.Sc. degree in Electrical and Electronic Engineering from the Islamic University of Technology (IUT), Gazipur, Bangladesh, in 2007, a M.Sc. degree in electrical engineering from the King Fahd University of Petroleum and Minerals (KFUPM), Dhahran, Saudi Arabia, in 2011 and a Ph.D. degree in Electrical and Electronic Engineering from the Islamic University of Technology (IUT), Gazipur, Bangladesh, in 2018. Currently, he is serving as an Associate Professor of Electrical and Electronic Engineering at the Islamic University of Technology (IUT), Gazipur, Bangladesh, a subsidiary organ of OIC in Bangladesh. His current research interests include the generation and application of high-power microwaves, modeling and simulation of high-frequency active devices, optically controlled active devices, computational electromagnetics, plasmonics and nonlinear integrated optics.